Heat Mass Transfer (2014) 50:933–943
DOI 10.1007/s00231-014-1306-4

ORIGINAL

Investigations of the reduction of NO to N_2 by reaction with Fe under fuel-rich and oxidative atmosphere

Janusz A. Lasek

Received: 21 January 2013 / Accepted: 30 January 2014 / Published online: 12 February 2014

Abstract The limitation of nitrogen oxides (NO_x) emissions from stationary combustion chambers is still an important issue in the field of the natural environment protection. This paper describes the reduction of NO_x in the presence of iron. A few new aspects of research describing the utilization of iron as an additive that influences NO_x reduction at high temperatures are presented. In particular, the influence of the excess air number (λ) on the NO_x removal efficiency in the presence of Armco iron was determined. A >50 % increase in the efficiency was achieved at $\lambda = 0.6$. The research was conducted using N_2/NO mixed with a flue gas from carbon monoxide combustion. In addition, a correction factor (Arrhenius-type empirical equation) was determined, which enabled the calculation of the oxygen influence on the inhibition of the de-NO_x reaction in the presence of iron. The NO_x reduction was also tested using bearing steel samples. Finally, the use of iron in de-NO_x processes under different combustion conditions is briefly reviewed and analyzed.

1 Introduction

Nitrogen oxides (NO_x) are harmful gases emitted from combustion processes. Different NO_x removal methods have been intensively investigated, and these methods can be differentiated into two main groups: primary and secondary measures [1, 2]. In primary measures, the combustion process is modified to obtain proper reducing conditions. The NO_x are eliminated inside the combustion zone, and thus the use of an additional reactor behind the main combustion zone is unnecessary. Examples of primary measures include fuel staging (reburning), air staging, exhaust-gas recirculation (EGR) and others. The main secondary measures are selective catalytic reduction (SCR) and non-selective catalytic reduction (NSCR).

The development of advanced low-emission methods (e.g., oxy-fuel combustion [1, 3, 4] or synergetic gasification–combustion systems [5]) will eventually decrease pollutant emissions (including NO_x). However, a current important problem is the abatement of NO_x emissions from traditional air-fired combustion chambers. Moreover, according to European Union legislation, the emission of NO_x must be significantly reduced before 2016 [6]. In addition, the U.S. Environmental Protection Agency (EPA) has underscored the still-important issue of NO_x emissions. The agency has established a new 1-h NO_2 standard at the level of 100 ppb and has encouraged the development of standards to limit the impacts of NO_x on ecosystems [7, 8]. Reburning technology is known as a cost-effective primary method of NO_x removal. The de-NO_x efficiency can be increased through the use of additional compounds, such as ammonia, urea or metals, that can be introduced simultaneously with the main reburning fuel. This modification is known in the literature as advanced reburning [9–11]. An application of ammonia can be risky because of ammonia slip, the build-up of ammonium salts on heat-transfer surfaces and the creation of ammonium chloride [1]; consequently, metallic iron has been proposed as an alternative additive in advanced reburning [9]. This low-cost compound is readily available; moreover, it does not negatively influence the combustion process.

A survey of the literature [12–14] suggests that relatively few studies on the reduction of NO_x in the presence of iron (or its oxides) have been reported. NO is assumed to be oxidized by metallic iron via the reaction:

J. A. Lasek (✉)
Institute for Chemical Processing of Coal, ul. Zamkowa 1, 41-803 Zabrze, Poland
e-mail: jlasek@ichpw.zabrze.pl

$$NO + Fe \rightarrow FeO + 1/2\ N_2. \quad (1)$$

In other words, the nitric oxide can be converted back to molecular N_2. Reaction (1) is therefore useful for the abatement of NO_x emissions. The product of the reaction, iron oxide, can be chemically reduced to metallic Fe via the reaction:

$$CO + FeO \rightarrow Fe + CO_2, \quad (2)$$

which can occur in fuel-rich regions of the combustion chamber. The net effect of reactions (1) and (2) is:

$$CO + NO \rightarrow CO_2 + 1/2\ N_2. \quad (3)$$

It should be noted that complete oxidation of Fe to Fe_2O_3 is possible for temperature range of 973–1173 K and NO concentration lower than 500 ppmv [15]. Table 1 shows calculation of Gibbs free energy. In all cases of iron oxidation products, spontaneous reaction is possible due to negative value of the Gibbs free energy.

The form of iron product is still discussed. It was recently discussed by Lasek and Gradon [16] and Su et al. [14]. Also other researchers confirmed that type of iron oxide (or oxides), created at NO presence, is still open question [12, 14, 17]. For example, Fennel and Hayhurst [17] concluded that main product of iron oxidation in NO/N_2 mixture may be magnetite (Fe_3O_4). Lasek and Gradon [18] confirmed this observation using Energy Dispersive Spectrometer (EDS) technique of iron oxide analysis along a cross-section of the oxide layer. Moreover, wustite (Fe_xO) formation is also possible because this phase is not stable at temperature below 572 °C and can be next decomposed into magnetite and iron [7]. Hayhurst and Lawrence speculated that the iron oxide is mainly FeO, with a small amount of Fe_2O_3 [19]. Su et al. [20, 21] found that iron oxides content depended on temperature range. They concluded that Fe_3O_4 was the major iron oxide at 550 °C and Fe_2O_3 was the major iron oxide at 1,100 °C. In another experiment, Su et al. [22] noticed that FeO, Fe_3O_4, Fe and Fe_2O_3 were formed in CO_2 atmosphere, but $Fe_3O_4$and Fe_2O_3 were formed when O_2 was added at temperature about 700 °C. Moreover, at higher temperature of 900 °C Fe_2O_3 was formed at the surface of the iron mesh. It is clear that type and morphology of created iron oxides in the scale depend on the oxidation conditions. Especially, temperature and oxidant gases composition in reaction system play predominant role.

Until now, research has primarily focused on the influence of other gaseous compounds (O_2, CO_2, CO, N_2O) with respect to NO removal efficiency in the presence of iron and on the morphology of the iron oxide layer created in the reaction with NO_x. Additionally, the kinetic coefficients of the chemical reaction between NO and Fe have been determined as a function of temperature [9, 13, 15, 17, 19, 23]. Recently, Fennell et al. [12] reported a study of the latter stages of reaction (1), when the process has been controlled by the diffusion of iron ions through an oxide layer around the iron particle. The research was performed using a thermogravimetric balance, and the authors concluded that iron or its oxides could be usefully included in a fluidized-bed combustor to remove NO_x. Su et al. [24] confirmed that the combination of fine Fe_2O_3 with scrap tires (as a reburning fuel) caused a significant decrease in NO_x emissions.

Metal cations (including Fe) are contained in coals as ion-exchanged forms, and these cations can change the partitioning of coal mass into gas, tar, and char upon pyrolysis. In addition, Fe cations catalyze the conversion of char-N to N_2 and, as a consequence, decrease NO_x emissions. This scientific problem has been addressed by Tsubouchi and Ohtsuka [25]. In addition, Illán-Gómez et al. [26] have observed that iron catalyzes the reduction of NO by carbon through an oxidation/reduction mechanism. The effect of the coal-ash content on the NO reduction efficiency in the coal reburning process has been investigated by Wang et al. [27]. Iron was recognized as one of the most effective compounds (in ash) that influenced the reburning efficiency. Although these issues are important, they are only mentioned to provide a clear explanation of the role of iron in NO formation/reduction processes during the combustion of solid fuels. The influence of the presence of iron in solid fuels on the conversion of NO has been not investigated in previous research.

Notably, little attention has been focused on the influence of process parameters, such as the oxygen concentration in the reaction zone, the excess air ratio and the iron impurity levels (alloying), with respect to the NO reduction efficiency in the presence of iron. If iron or its oxides are destined to be used in real-scale industrial combustion

Table 1 Calculation of Gibbs free energy (using JANAF tables) for oxidation of Fe in NO presence

T, K	$Fe + NO \rightarrow FeO + 1/2N_2$ $\Delta_fG°$	$Fe + 4NO \rightarrow Fe_3O_4 + 2N2$ $\Delta_fG°$	$2Fe + 3NO \rightarrow Fe_2O_3 + 3/2N_2$ $\Delta_fG°$
1000	−284.73	−1,103.702	−795.191
1100	−277.178	−1,068.495	−766.695
1200	−269.555	−1,033.095	−738.091
1300	−261.916	−997.647	−709.469

chambers, these unexplored issues should be taken into account. Usually, investigations are preliminarily performed using laboratory-scale equipment, and this approach has therefore been adopted in this research. However, the results can be useful in applying this technology in real-scale processes, as suggested by Fennell et al. [12]. In this paper, some aspects of the practical application of iron (as Armco iron or steel) for NO_x removal are presented. This work complements and continues our previous study [13]. In particular, the influence of excess air on the de-NO_x efficiency in the reaction with Fe during CO combustion is determined. In addition, an empirical correction factor that takes into account the influence of oxygen on the efficiency of the de-NO_x process is proposed. Additionally, the NO reduction is investigated in the presence of oxygen and bearing steel samples. The application of iron in de-NO_x processes under different conditions is briefly discussed.

2 Experimental

The experimental setup was similar to that described in our previous work [13]. Investigations were performed in an externally heated cylindrical ceramic reactor with an inside diameter of 18 mm and with a heating zone 380 mm in length. In some experiments (exhaust-gas conditions), a ceramic element was placed behind the inlet gas pipe for flame stabilization. The vertical cross section of the experimental setup is presented in Fig. 1.

Four spherical, non-porous iron or bearing steel samples with diameters of approximately 10 mm were placed in the center of the reactor. The spheres in the reactor were arranged on a thin ceramic plate such that they had only point contact with the ceramic base. Table 2 presents the chemical composition of iron measured using a spark spectrometer (ARL 2460 Thermo Scientific). The chemical composition of typical Polish bearing steel alloy (for making balls with diameters of <30 mm) is presented in Table 3 [28].

The total surface area of the samples was approximately 1.25×10^{-3} m^2. The differences between the surface areas of the iron and bearing steel samples were caused by polishing the samples before the experiment. Mixtures of NO (1,015 ppm)/N_2, NO/O_2/N_2, and NO/CO/air ($\lambda = 0.6$–1.3) were continuously supplied to the reactor; when the gases exited the other end, they were cooled and passed through a calibrated electrochemical analyzer (Testoterm testo 350), which continuously measured the concentrations of NO and NO_2. The uncertainty in the NO measurements was <5 ppm. Air was supplied from a pressure pump, and carbon monoxide and oxygen were supplied from cylinders. The gases, before entering the reactor, were well mixed using a glass element, and their streams were stabilized and measured using rotameters and flow controllers, with an uncertainty margin of 2.5 %.

The experimental course was similar to earlier research [13]. At the beginning of each experiment, the samples were placed into a cold reactor, and the system was subsequently heated to the proper temperature. Nitrogen (99.999 % purity) flowed through the reactor during the heating period (i.e., until the moment when a fixed and uniform temperature in the whole volume of the iron samples was achieved). After the heating period, the nitrogen flow was turned off, and the mixture of 10 vol% CO in N_2 was supplied into the reactor for approximately 10 min to remove possible small quantities of iron oxides that may have been formed during the brief contact of the samples with atmospheric air. The system was subsequently purged with N_2, and the proper gas mixture that contained NO was fed into the reactor. The temperature was measured using a removable Pt-RhPt thermocouple placed in the center of the reactor. During previous experiments [13, 29] in which a similar reactor technique was used, the temperature measured in this way was found to represent the reactor wall temperature. Thus, the temperatures of samples and the heating period were evaluated on the basis of a measured value based on heat transfer equations solved numerically. The combustion of the carbon monoxide did not significantly influence the

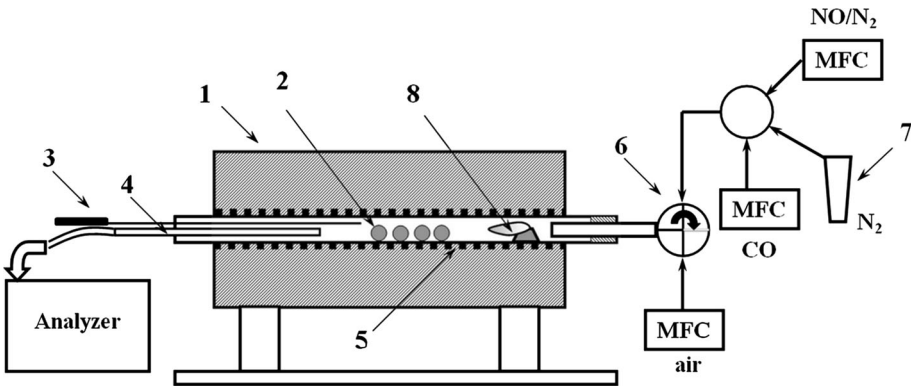

Fig. 1 Experimental setup used in experiments under exhaust-gas atmosphere: *1* furnace, *2* samples of iron or bearing steel, *3* thermocouple, *4* gas probe, *5* heating elements, *6* three-way valve, *7* rotameter, *8* ceramic element for flame stabilization, *MFC* mass flow controller

Table 2 Chemical compositions of the iron samples used during the investigations

Chemical element	Average content, %	Chemical element	Average content, %
C	0.03	Ti	0.002
Mn	0.13	Al	0.06
Si	0.02	Cu	0.05
P	0.004	As	0.003
S	0.22	Co	0.007
Cr	0.1	Nb	0.000
Ni	0.02	B	0.0005
Mo	0.01	Sn	0.004
W	0.01	Pb	0.0017
V	0.00	Fe	99.3

Table 3 Chemical compositions of typical polish bearing steel alloy [28]

Steel	Average content of chemical compounds, %					
	C	Mn	Si	P	S	Cr
ŁH15	0.95	0.4	0.3	0.027	0.020	1.30

temperature change because the maximum power of the burner (calculated from the chemical energy of the carbon monoxide) was 31.4 W. The ratio of the furnace power to the burner power was >25 for this fuel. The excess air number λ was calculated basing on the streams of gas reactants. The streams of NO/N_2 and air were maintained at constant levels (0.9 l/min (STP) and 0.25 l/min (STP), respectively), and the CO stream was varied in the range of 0.094–0.176 l/min (STP). The superficial gas velocity varied with the temperature from 0.3 to 0.46 m/s. The residence time of the process gas in the reaction zone (iron/steel existing) was in the range of 0.1–0.15 s. The NO molar fraction was measured at the outflow of the reactor as a function of time at a temperature of 850 °C. The temperature range for experiments with a model gas atmosphere that included $NO/O_2/N_2$ was 850–1,000 °C. Figure 2 shows the flame stabilized by a ceramic element.

3 Results and discussion

3.1 Fuel-rich atmosphere

Figure 3 shows an example of the experimental results for the combustion of CO in the presence of iron. The figure depicts the measured NO concentration in the outlet of the reaction chamber as a function of the excess air ratio, λ. The λ number was periodically changed through the use of different streams of carbon monoxide. The solid line

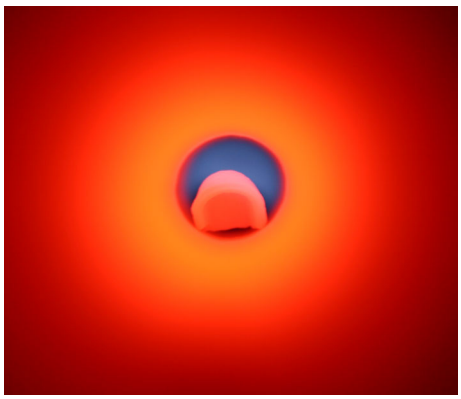

Fig. 2 The flame stabilized on a ceramic element during carbon monoxide combustion

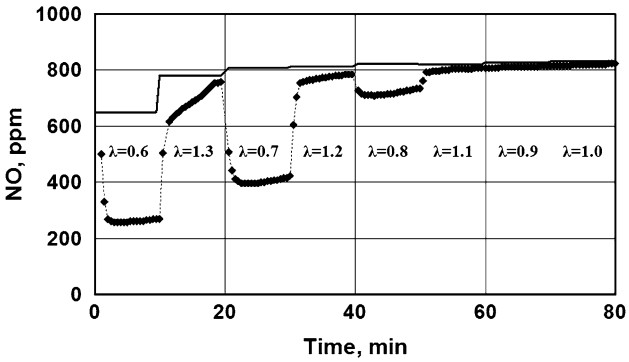

Fig. 3 Reduction of NO during CO combustion at different excess air ratios (λ). (*thin line*) the NO_x fraction measured for the empty reactor; (*Diamond*) the NO fraction measured for the reactor loaded with Armco iron samples (four spherical samples, $A = 1.14 \times 10^{-3}$ m^2), 850 °C

represents the NO concentrations measured for an empty reactor with a ceramic plate for the iron samples. The points on the dashed line show the NO concentration measured for the reactor loaded with iron. Thus, only the influence of the iron on the de-NO_x process is assumed to have been taken into account, i.e., the results show the influence of the iron on NO_x abatement in fuel-rich and fuel-lean exhaust gas atmospheres.

The effect of NO reduction by homogeneous reaction with CO was neglected in the calculations. The influence of the aforementioned reaction on the NO conversion was intentionally omitted to emphasize the role of iron as an additive that supports the reburning process. The experiments were performed this way because the influence of temperature, reburning fuel type, reburning fuel heat input and other process parameters on the efficiency of NO reduction has already been intensively investigated [30–33], whereas relatively few studies on the influence of iron on the reburning efficiency have been published [9, 14, 23, 24]. The efficiency of NO_x reduction in the presence of iron

as a function of the excess air numbers was calculated according to Eq. (4):

$$\eta = \left(1 - \frac{z_{NO_x iron}}{z_{NO_x empty}}\right) 100\,\% \quad (4)$$

where $z_{NO_x iron}$ represents the volumetric NO_x fraction measured in the case of a reactor loaded with the iron sample, and $z_{NO_x empty}$ represents the volumetric NO_x fraction measured for an empty reactor. The results are shown in Fig. 4.

The motivation for the use of carbon monoxide was the potential application of alternative gases in the reburning process. Recently, the gas from biomass gasification has been recognized as a highly effective reburning agent. It is also worth noting that the high concentration of CO included in this fuel [30, 31]. For example, the integration of a coal-fired boiler with a biomass gasifier has been used in a thermal power plant in Zeltweg, Styria-Austria [34]. Moreover, a high concentration of CO is observed in fuel-rich zones of stages combustion, e.g. of the Rich-burn/Quick–mix/Lean-burn (RQL) combustor, reported by Samuelsen et al. [35]. A positive interaction between iron and CO in terms of reduced NO_x emissions (see Eqs. 1–3) provides a good perspective for the use of alternative fuels with respect to, e.g., gasification products or blast furnace gas. In addition, fuel-rich zones are created when staged combustion (fuel/air-staging) is applied in a grate chamber. A large reduction in NO_x emissions was achieved via staged combustion at a temperature of approximately 850 °C; thus, the use of iron waste in this type of combustion chamber is worth consideration. As shown in Fig. 4, the decrease in λ caused an enhancement of the iron influence because the contribution of the reducing component, carbon monoxide, enhanced the overall reaction (3); i.e., the iron particles can play the role of a catalyst for NO reduction. However, the reaction can occur in the combustion zone without the use of an additional reactor [12, 13, 17].

As evident from the results in Fig. 4, favorable conditions for the utilization of iron in the de-NO_x process are created in fuel-rich atmospheres. Lissianski et al. [9] reported a similar trend using a pilot-scale boiler system. The pulverized coal and natural gas were used as the main fuel. The reburning was achieved through the application of natural gas, and the reburning level was maintained at 18 and 25 % of the total heat input, calculated according to the main fuel. The volumetric fractions of carbon monoxide in the reaction zone were obtained from model calculations (0.3 and 3.7 vol % for 18 and 25 % reburning, respectively) at 1,320 °C. The injection of iron improved the process efficiency by 8–10 %. The maximum achieved efficiency was 85 % when reburning and iron injection were applied. Although the application of iron for NO_x reduction is preferred for fuel-rich conditions (reducing zones at air or fuel staging processes), positive results can also be achieved when the iron is introduced into a fuel-lean zone. Lissianski et al. [9] reported increased NO_x reduction (a de-NO_x efficiency of 23 %) when only iron was injected directly into the combustion zone, without reburning. In another test, the iron waste was co-injected with a small amount of the reburning fuel (approximately 6 %); thus, the total composition of the mixture was fuel-lean. In this case, the NO_x reduction increased from 32 (only reburning) to 38 %. Figure 5 shows the change in the de-NO_x efficiency as a function of time when the excess air ratio was rapidly changed from 0.6 to 1.3. As evident in Fig. 5, after more oxygen was introduced and the conditions were changed from fuel-rich to fuel-lean, the de-NO_x efficiency decreased from approximately 60 % to almost zero. However, the decrease in the efficiency was extended over time. Evidently, NO_x reduction is still possible when the iron is introduced under fuel-lean conditions. Of course, to achieve a relatively high NO_x reduction, the residence time of the iron particles should be optimized, i.e., this time cannot be too long because the de-NO_x

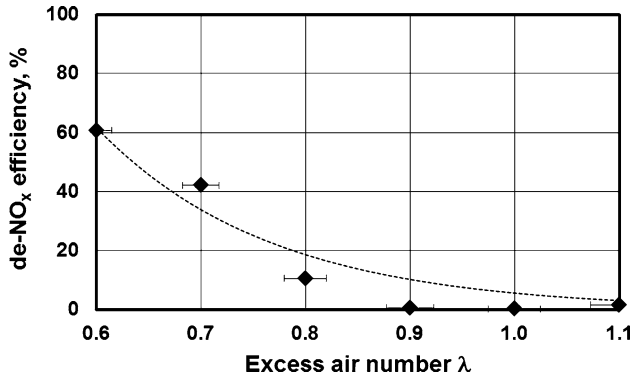

Fig. 4 The efficiency of NO reduction during the combustion of carbon monoxide in the presence of iron for different excess air ratios (four spherical samples, A = 1.14×10^{-3} m^2), 850 °C

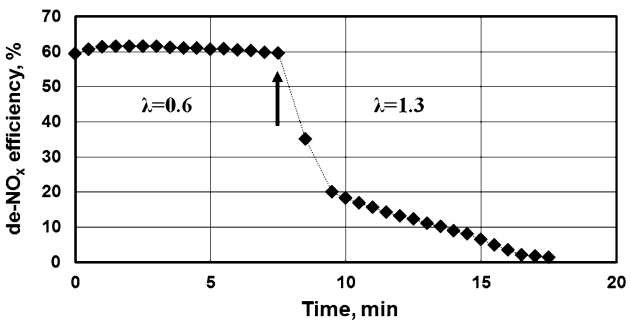

Fig. 5 Influence of excess air ratio (λ) on the de-NO_x efficiency at 850 °C for carbon monoxide combustion; the iron surface area was 1.14×10^{-3} m^2. The *arrow* shows a step change of the λ during the experiment

process is inhibited in the presence of oxygen. The reason for this inhibition is the creation of a relatively thick and highly resistive (diffusion) iron oxide layer. The efficiency depends on the process parameters; in particular, the concentration of oxygen in the combustion zone appears to be the most crucial parameter. This aspect is discussed in the next section.

3.2 Correction factor that accounts for the oxygen influence

Gradoń and Lasek [13] investigated the influence of oxygen on the inhibition of de-NO_x efficiency when iron was present. They concluded that the presence of 4.5 vol% of O_2 caused a decrease in the NO reduction efficiency to zero when the residence time of the iron samples was longer than 5 min. Undoubtedly, NO reduction at iron presence and fuel-rich regions is more efficient, however, a reduction of NO in the presence of oxygen is possible if the residence time of the iron samples in a lean exhaust gas atmosphere is sufficiently short. In this research, the experimental data were complemented, and the experiments were performed under similar flow conditions at 2 vol% O_2 and in the temperature range 850–1,000 °C. Based on these results, an empirical factor (Eq. 5) was determined that allowed the calculation of the influence of oxygen on the de-NO_x process inhibition. This approach is similar to the determination of the time-dependent factor that describes a catalyst decay process, as described in Fogler's work (p. 717) [36]. In addition, this equation (Eq. 5) has been adopted because this form is mathematically consistent in cases where the oxygen concentration is zero, i.e., when the oxygen molar fraction $z = 0$ is substituted into the equation, the k_{rNO-O2} parameter equals the k_{rNO} value estimated from previous research [13].

$$k_{rNO-O_2} = k_{rNO} \exp\left(-\frac{tz}{A_1}\right) \tag{5}$$

The overall process rate coefficient k (m/s) is defined by the formula $1/k = 1/k_{rNO-O2} + 1/k_g$, where k_g is the mass transfer coefficient. The empirically determined k_{rNO-O2} parameter is assumed (by a simplification) to include both the rate of the chemical reaction and the diffusion of compounds by an iron oxide layer created during the process. The $k_{rNO} = 0.527exp(-13/RT)$ (m/s) expression used in Eq. 5 represents the rate constant (first order in NO) of the reaction between NO and Fe determined in previous research [13]; t is time in s, z is the volumetric fraction of O_2 (as the total value, e.g., 1 % should be used as 0.01), and $A_1 = 1.58$ s. The overall rate constant k was obtained from the balance of NO, $\dot{R} = \dot{V}\left(C'_{NO} - C''_{NO}\right) = kA_{Fe}C_{NO}$, where $\dot{V}$ is the gas stream flowing through the reactor (m^3/s), and C'_{NO} and C''_{NO} are the NO concentrations (mol/m^3) at the reactor inlet and outlet, respectively. The k_{rNO} is slightly different comparing to previous study [13]. A mass transfer coefficient was calculated using the equation of Thoenes and Kramers equation for a packed bed system [13]: $\frac{Sh\phi}{(1-\phi)\gamma} = \left[\frac{Re}{(1-\phi)\gamma}\right]^{0.5} Sc^{0.33}$, where the Reynolds number is defined as $Re = w_g\rho_g d/\eta$, and the Schmidt number is defined as $Sc = \eta/\left(\rho_g D_{NO-N_2}\right)$. Here, D_{NO-N2} is the diffusion coefficient for NO in N_2; w_g, ρ, and η are the velocity, density and viscosity of the gas flowing through the reactor, respectively; ϕ is the void fraction of the packed bed; and γ is the shape factor of the iron particle (for spherical particles, $\gamma = 1$). The range of the Reynolds number was 26.3–21.2, and the range of the Schmidt number was 0.73–0.74. This calculation gave overestimated values. Simplified discussion of other correlations is shown in Table 4. For estimation of k_g coefficient in this research Gnielinski [37] was used (see in Table 4). This correlation is more complicated (comparing to other equations) however, according to Tsotsas and Schlunder [37] explanation this equation is applicable in different bed systems, regular and distended packings and to single particle as well. Wakao and Funazkri correlation would be applicable correlation for other bed porosity. As it was reported by Tsotsas and Schlunder [37] it can be applied only to monodispersed random beds of spherical particles at a void fraction about $\phi = 0.4$. Dwidevi Upadhyay [36] correlation is more all-purpose application, however, Gnielinski is more specific for the system used in this research.

The overall rate of NO_x reduction is inhibited because it is controlled by the internal diffusion in a later stage of the process. This phenomenon is described in the literature [12, 15]. According to the explanation provided in the literature, the oxidation of iron in the presence of oxygen (a later stage) is controlled by the diffusion of iron ions from the unreacted metal core to the external surface of the metal oxide. However, during the oxidation of iron by NO, a porous and almost sponge-like layer of oxide is created [13]. Therefore, in the case of the complex system of NO + O_2, the process can be controlled by the diffusion of iron ions and simultaneously by the diffusion of molecular oxygen and nitric oxide from the bulk phase through boundary and sponge-like oxide layers to the unreacted metal core. However, during the latter stages of the reaction between NO and Fe, the process is instead controlled by the diffusion of iron ions through an oxide layer [12]. The particular mechanism of NO_x reduction is complicated; thus, the use of the "decay law" (Eq. 5) to describe the de-NO_x process appears to be a reasonable solution. This equation can be very useful in modelling and engineering calculations when Fe will be considered as a compound that influences the NO_x reduction in the oxygen-

Table 4 Comparison of mass transfer correlations (for packed bed) analyzed in this research, calculated for conditions: particle diameter of 1 mm, T = 850 °C, w_g = 0.35 m/s

Correlation	Equation	Conditions	k_g, m/s
Dwidevi Upadhyay	$\phi \frac{Sh}{Sc^{1/3}Re} = \frac{0.765}{Re^{0.82}} + \frac{0.365}{Re^{0.386}}$	$Re > 10$	0.0393
Gnielinski	$Sh = f_\psi \left[2 + \sqrt{Sh_1^2 + Sh_2^2}\right]$ $Sh_1 = 0.664 Re^{1/2} Sc^{1/3}$ $Sh_2 = \frac{0.037 Re^{0.8} Sc}{1+2.443 Re^{-0.1}(Sc^{2/3}-1)}$ $f_\psi = 1+1.5(1-\psi)$ Re number is calculated for void fraction as Re_0/ψ	$2.4 < Re < 1{,}500$	0.0498
Wakao and Funazkri	$\mathrm{Sh} = 2 + 1.1\mathrm{Re}^{0.6}\mathrm{Sc}^{1/3}$	$3 < Re < 3{,}000$ $0.5 < \mathrm{Sc} < 10000$	0.0770

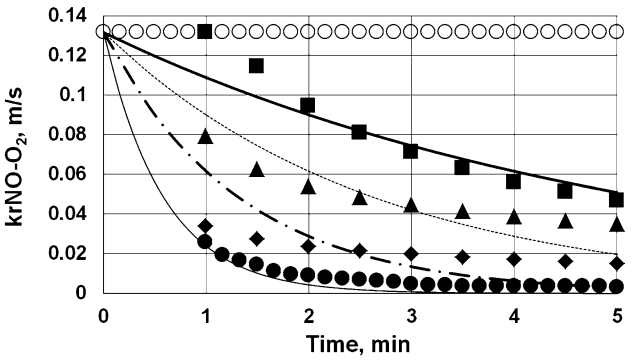

Fig. 6 A comparison of the kinetic rate constant calculated from experimental data (*points*) and those calculated from the model Eq. 5 (*lines*). Conditions: T = 850 °C, average iron surface area 1.16×10^{-3} m^2, *open circle* 0 % O_2 ($k_{rNO} = 0.527 exp(-13/RT)$), *filled square* 0.5 %, *filled triangle* 1 %, *diamond* 2 %, and *filled circle* 4.5 % O_2; *thick line* 0.5 %, *dashed line* 1 %, *dotted line* 2 %, and *thin line* 4.5 % O_2

rich zones. A comparison between the model calculations and the experimental results is shown in Fig. 6.

3.3 Bearing steel

The oxidation rate of iron depends on alloy impurities included in the iron structure. The existence of metals such as chromium, aluminum and silicon are known to provide a certain level of oxidation resistance; however, this effect is not significant if the amount of the alloying element is relatively low. In addition, carbon, as a main alloy element of steel, can suffer decarburization during steel oxidation, which inhibits the oxidation rate [38]. How the alloying elements included in steel influence the de-NO_x efficiency remains an unresolved issue. This research question is important for the potential application of low-alloy steel waste for the abatement of NO_x emissions. In this research, the efficiency of the NO reduction in the presence of Armco iron and bearing steel was compared. The experiment was performed using a model gas atmosphere that contained 1,015 ppmv NO in N_2 and 880 ppmv NO/3.2 vol% O_2 in N_2. Figure 7 shows the comparison of the efficiency of NO removal using Armco iron and bearing steel samples. The efficiency in the case of the bearing steel is lower because the alloy elements decreased the oxidation rate of the steel samples. As evident from the results in Table 2, bearing steel is not a high-alloying material. The mass fraction of each alloy element does not exceed 1 wt%. The influence of chromium (included in the bearing steel) on the kinetic rate of the steel appears to be negligible. High corrosion-protective properties are known to be obtained when more than ~16 wt% of Cr is included in the steel as an alloy element; thus, the influence of the chromium on the de-NO_x process appears to be insignificant. However, relatively small silicon additions are known to have beneficial effects on the oxidation resistance of steels because of the formation of a layer of silica adjacent to the metal [8]. Thus, more attention should be placed on the influence of silicon on the de-NO_x process. Silicon was shown to contribute to the creation of a compact oxide layer that inhibited the corrosion process [28]. Suárez et al. [39] confirmed that an inhibition of iron oxide growth was caused by the presence of silicon in bearing steel. Suárez et al. attributed this inhibition to the influence of a fayalite ($FeO{\bullet}2SiO_2$) phase that was created on a metal–oxide interface; this phase reduced the diffusion of iron ions that control the growth of the oxide layer. The presence of carbon decreased the oxidation rate compared to that of pure iron, and the authors observed that the decarburization process was significant at 850 °C. The lower oxidation rates were attributed to the rejection of carbon at the scale–alloy interface, which caused poor contact between the scale and the alloy; however, when the oxidation times were short, the scale structures were similar to those formed on iron [38]. Thus, this description provided in the

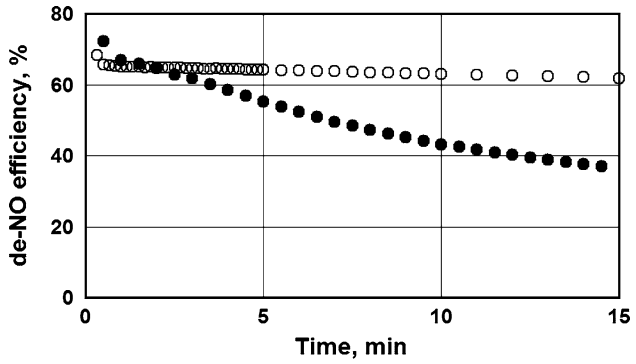

Fig. 7 Comparison of de-NO_x efficiency in the presence of Armco iron *open circle* (four spherical samples, A = 1.21 × 10^{-3} m^2) and bearing steel *filled circle* (four spherical samples, A = 1.25 × 10^{-3} m^2) as a function of time. The gas atmosphere contained 1,015 ppm NO/N_2, T = 850 °C

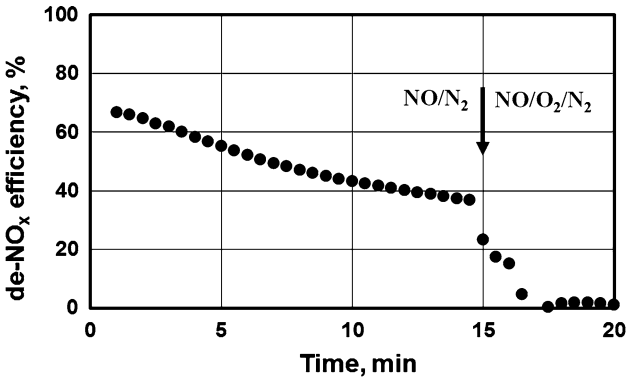

Fig. 8 Influence of oxygen (3.2 % molar fraction) on the NO reduction efficiency at 850 °C in the presence of bearing steel samples with a surface area of 1.25 × 10^{-3} m^2. The *arrow* indicates the moment when oxygen was added to the 1,015 ppm NO/N_2 mixture

literature explains why the de-NO_x efficiency is almost the same in the cases of iron Armco and bearing steel in the first minutes of the process (see Fig. 7). After 5 min of the process, the difference between the de-NO_x efficiency in the presence of iron and bearing steel increased as the oxidation process progressed. However, after 10 min of the process, the de-NO_x efficiency in the presence of bearing steel samples was still >40 %. Thus, even when this type of steel is present in iron waste, it can still be used as a de-NO_x agent.

The influence of alloy compounds on the de-NO_x process in the presence of steel has not yet been closely investigated. Only a few comments on it can be found in the literature. Lissianski et al. [9] tested different iron-containing additives for the control of NO_x emissions. Iron and iron waste were suggested as compounds that induce a decrease in the emissions; however, the authors did not explain exactly what type of iron waste (steel) was used. They noted only that the samples came from the steel processing industry and consisted nominally of approximately 80 % Fe_2O_3 and 20 % impurities, mainly $Ca(OH)_2$. Approximately 80 % of the particles were smaller than 50 μm in diameter. The bearing steel was tested in the current study to determine the potential influence of alloy compounds on the de-NO_x process. The addition of the mentioned compounds (silicon and carbon) to iron waste is possible (not expensive) because these compounds can occur in low-alloy steels. It has been already mentioned that their corrosion inhibition activity is relatively high [39]. The influence of other compounds, such as chromium, is also interesting; however the use of high-alloy steel for NO_x reduction (as an active compound introduced directly with a fuel) is not a reasonable solution because of its relatively high price and because important constituents of the alloy could be lost after the alloy is introduced into the combustion zone. Similar to Lissianski's suggestion [9], it is assumed that iron waste is introduced into the combustion zone and then removed as an ash. Notably, Sadakata et al. [40] have proposed stainless steel (18.3 wt% Cr and 9.3 wt% Ni) as an active compound for NO_x reduction; however, this system represents a secondary method. This solution requires an additional reactor when the stainless steel is used as a honeycomb-type catalyst, and the reaction is performed at a higher concentration of CO (2.7 vol%) and H_2 (2.4 vol%).

From an application perspective, the influence of oxygen on the de-NO_x efficiency when bearing steel is used as a de-NO_x agent is significant. Figure 8 depicts the results of the experiment when oxygen (from air) was immediately introduced into a NO/N_2 system. The efficiency decreased rapidly when the oxygen (3.2 vol%) was introduced into the reaction zone, and the rate of activity decay was higher than that for Armco iron. At 950 °C and 4.5 vol% O_2, the de-NO_x efficiency decreased after approximately 5 min of exposure to a $NO/O_2/N_2$ atmosphere [13]. The higher rate of de-NO_x inhibition was most likely caused by the influence of silicon (alloy element) on the oxidation process.

3.4 Application of iron in the de-NOx process: a brief analysis

As previously mentioned, only a few published studies on the use of iron for the de-NO_x process have been reported in the literature. Based on the literature data, the iron or its alloys can be used in both fuel-rich and fuel-lean atmospheres; however, the reducing atmospheres (fuel-rich) are preferred because of the positive effect of carbon monoxide. Notably, iron or its compounds (alloys, oxides) can be used for the de-NO_x process in two types of methods: primary and secondary methods. The application of iron

(or/and its alloys/oxides) as a catalyst (secondary measures) in a separate reactor (similar to the concept of selective catalytic reduction, SCR) has been previously proposed [40–44]. For example, Randall et al. investigated the reduction of NO and N_2O by CO over silica-supported iron oxide (Fe_2O_3 or Fe_3O_4) catalysts. The reactions were performed at T = 310 °C and at an elevated pressure (150 kPa). However, in the current study, the iron (or low-alloy steel) is suggested to be directly introduced (together with a fuel) to the main or the reburn combustion zone, similar to other studies [9, 12–15, 17, 19, 23, 24, 30]). Table 5 shows a comparison of the use of iron in the reburning process. Only the influence of iron (without reburning reactions) was taken into account. Undoubtedly, the mentioned combustion chambers are characterized by different process parameters (e.g., the type of fuel, the combustor, the temperature and others); thus, this comparison provides only a simplified analysis. However, these results are interesting because they clearly show that iron or iron oxides can be used in a wide range of combustion conditions. Lissianski et al. [9, 23, 30], who used a pilot-scale combustion chamber, and Su et al. [24], who used a laboratory-scale facility, both focused on the use of iron or iron oxide in pulverized coal combustion chambers. Fennel et al. [12, 17], who used the TGA method, Hayhurst and Lawrence [19], who used a laboratory-scale FB reactor, and Hayhurst and Ninomiya [15], who used a laboratory-scale FB reactor, suggested the use of iron as a de-NO_x agent in fluidized-bed combustors. Although some necessary model simplifications have been adopted, the results obtained in this work can be assumed to be useful for the application of iron as the active species for NO_x removal from grate combustion chambers. The particles used in this research are large; thus, the iron waste can be used (size >1 mm) in a real-scale chamber. In addition, parameters such as the temperature range (800–1,000 °C), the gas velocity (below 1 m/s), and the residence time of solid compounds (iron activity >3 min) were similar in this type of chamber [45–47].

Iron can also be effectively used in fuel-lean combustion zones. Both of the previously mentioned zones—fuel-lean and fuel-rich zones—exist in grate boilers. Based on the description of grate-boiler technology provided by Yin et al. [46], precise control of these zones can be attained using an advanced secondary air supply system. The local stoichiometry in the combustion zones plays a particularly important role for the effective utilization of iron as a de-NO_x agent. The possible and precise control of the residence time [46] can enhance the efficiency of NO_x reduction. Normann et al. [1] compared different de-NO_x methods with respect to oxy-fuel combustion. Their analysis was based on practical experience under air-fired conditions and/or modelling/experiments under oxy-fuel conditions. The use of different de-NO_x methods (primary and secondary) was possible; however, as the researchers concluded, the use of both methods requires the optimization of parameters, such as the combustion efficiency and economic issues, among others. The application of iron as the de-NO_x agent in oxy-fuel technology is also assumed to be possible and worth consideration. The CO_2 concentration in flue gas is known to be significantly higher (>80 %) compared to the exhaust gases in air-fired technology. However, at temperatures <1,000 °C, the rate of iron oxidation by CO_2 has been found to be at least 5–10 times lower than the rate of oxidation by O_2 [48]. Gradon and Lasek [13] observed no influence of CO_2 on the rate of NO destruction in their investigated temperature range of 750–1,200 °C. In addition, higher CO concentrations have

Table 5 A simplified comparison of reburning enhancement by the introduction of iron or its oxides into the reaction zone

Maximal increase in reburning efficiency due to the presence of iron	Type of iron samples, units and conditions	References
21 %	Iron waste (1,000 ppm, fine particles, 80 % smaller than 50 μm) or Fe_2O_3 (1,000 ppm, powder, smaller than 5 μm, 7.2 m^2/g), pilot scale (300 kW_t) boiler simulator facility, natural gas as reburning fuel at reburning heat inputs of 18 and 25 % from the total heat input, 1,320 °C	[9]
11 %[a]	Fe_2O_3 powder (99 % d < 5 μm), 4,000 ppm Fe, laboratory-scale tube reactor (internal diameter of 1.91 cm, total length of 30.48 cm), methane as a main and a reburning fuel (stoichiometric ratios in the reburning and burnout zones of 0.9 and 1.1, respectively), 1,250 and 1,150 °C for the reburn and burnout zones, respectively	[24]
60 %	Armco iron samples (10 mm, 1.25×10^{-3} m^2), carbon monoxide combustion at an excess air ratio of 0.6, 850 °C	This work

[a] The maximal de-NO_x improvement was >32 % when corn stover residue was applied as a fuel

been observed during oxy-fuel combustion [3]. The presence of the iron probably decreases the CO emissions from oxy-fuel processes due to the influence of the reaction (2). Thus, the use of iron as a de-NO_x agent in oxy-fuel combustion is worth consideration; however, it requires more specific investigations.

4 Conclusions

Improvements in de-NO_x methods are still a challenge for scientists and research engineers. The advanced reburning method appears to be a viable solution for the abatement of NO_x emissions, especially from common air-fired combustion chambers. These methods can be used in real-scale combustion systems (boilers and others). Metallic iron or low-alloy steel waste can be directly introduced into the combustion zone as effective de-NO_x agents. Based on these research results and literature data, the following conclusions are made:

The excess air ratio (λ) strongly influences the efficiency of NO reduction in the presence of iron. This influence is caused by the creation of preferential conditions for NO reduction on the iron surface.

A correction factor that accounts for the influence of oxygen on de-NO_x efficiency has been proposed. The coefficient is expressed by the equation $k_{rNO-O2} = k_{rNO}exp(-tz/1.58)$. The exponential form has been adapted from the catalyst decay law. This coefficient can be used for modelling NO reduction in the presence of iron and oxygen as well as for estimating the de-NO_x efficiency when iron is introduced into an oxygen-rich combustion zone.

Low-alloy steels waste can be used as an efficient de-NO_x agent. The tests (performed using bearing steel samples) show that NO_x can be effectively reduced in the presence of this agent; however, the alloy compounds inhibited the reduction of NO_x.

Based on literature data and on the results provided in this research, the application of iron in fluidized-bed, pulverized and grate combustors is sensible and worth consideration. The most preferable conditions for obtaining high efficiency are the use of iron or low-alloy steel waste in fuel-rich combustion zones. However, a reduction of the NO_x is also possible in oxygen-rich zones if the residence time of iron particles is sufficiently short.

Acknowledgments This work was supported by The Ministry of Science and Higher Education in Poland under Project Number 3 T10B 031 30 and by the Research and Development Strategic Program "Advanced Technologies for Energy Generation" Project No. 2 "Oxy-combustion technology for PC and FBC boilers with CO2 capture", supported by the National Centre for Research and Development, agreement No. SP/E/2/66420/10. The support is gratefully acknowledged. Additionally, I am grateful to Prof. Bogusław Gradoń, Prof. Jarosław Zuwała and Krzysztof Głód for their help during the research.

References

1. Normann F, Andersson K, Leckner B, Johnsson F (2009) Emission control of nitrogen oxides in the oxy-fuel process. Prog Energy Combust Sci 35(5):385–397
2. Roy S, Hegde MS, Madras G (2009) Catalysis for NOx abatement. Appl Energy 86(11):2283–2297
3. Toftegaard MB, Brix J, Jensen PA, Glarborg P, Jensen AD (2010) Oxy-fuel combustion of solid fuels. Prog Energy Combust Sci 36(5):581–625
4. Hashemi SA, Fattahi A, Sheikhzadeh GA, Mehrabian MA (2012) The effect of oxidant flow rate on a coaxial oxy-fuel flame. Heat Mass Transfer 48(9):1615–1626. doi:10.1007/s00231-012-1008-8
5. Sugiyama S, Suzuki N, Kato Y, Yoshikawa K, Omino A, Ishii T, Yoshikawa K, Kiga T (2005) Gasification performance of coals using high temperature air. Energy 30(2–4):399–413. doi:10.1016/j.energy.2004.06.001
6. II position of the european parliament (2010). EP-PE_TC2-COD(2007)0286, vol EP-PE_TC2-COD(2007)0286
7. Król L (1983) Redukcja bezpośrednia rud żelaza. Wydawnictwo Śląsk, Katowice
8. Evans HE, Hilton DA, Holm RA, Webster SJ (1983) Influence of silicon additions on the oxidation resistance of a stainless steel. Oxid Met 19(1):1–18. doi:10.1007/bf00656225
9. Lissianski VV, Maly PM, Zamansky VM, Gardiner WC (2001) Utilization of iron additives for advanced control of NOx emissions from stationary combustion sources. Ind Eng Chem Res 40(15):3287–3293. doi:10.1021/ie010019q
10. Nimmo W, Patsias AA, Hampartsoumian E, Gibbs BM, Fairweather M, Williams PT (2004) Calcium magnesium acetate and urea advanced reburning for NO control with simultaneous SO2 reduction. Fuel 83(9):1143–1150
11. Tree DR, Clark AW (2000) Advanced reburning measurements of temperature and species in a pulverized coal flame. Fuel 79(13):1687–1695
12. Fennell PS, Dennis JS, Hayhurst AN (2011) Latter stages of the reduction of NO to N2 on particles of Fe while simultaneously oxidizing Fe to its oxides. Energy Fuels 25(4):1510–1520. doi:10.1021/ef101675j
13. Gradon B, Lasek J (2010) Investigations of the reduction of NO to N2 by reaction with Fe. Fuel 89(11):3505–3509
14. Su Y, Deng W, Shen H (2012) Catalysis reduction of NO and HCN/NH3 during reburning: a short review. Adv Mat Res 354–355:365–368. doi:10.4028/www.scientific.net/AMR.354-355.365
15. Hayhurst AN, Ninomiya Y (1998) Kinetics of the conversion of NO to N2 during the oxidation of iron particles by NO in a hot fluidised bed. Chem Eng Sci 53(8):1481–1489
16. Lasek J, Gradoń B (2013 (in press)) Nitrous oxide destruction in contact with metallic iron. Combust Sci Technol. doi:10.1080/00102202.2013.819858
17. Fennell PS, Hayhurst AN (2002) The kinetics of the reduction of NO to N2 by reaction with particles of Fe. Proc Combust Inst 29(2):2179–2185
18. Lasek J, Gradoń B (2009) Możliwości wykorzystania żelaza i jego związków w niektórych działaniach na rzecz ochrony środowiska. Hutnik- Wiadomości Hutnicze 76(11):813–819

19. Hayhurst AN, Lawrence AD (1997) The reduction of the nitrogen oxides NO and N2O to molecular nitrogen in the presence of iron, its oxides, and carbon monoxide in a hot fluidized bed. Combust Flame 110(3):351–365
20. Su YX, Ren LM, Deng WY (2013) Effect of CO/CH4 on redox of iron during NO reduction by XRD/SEM. Appl Mech Mater 448–453:559–563
21. Su Y, Su A, Cheng H (2013) Experimental study on effect of CO on NO reduction by iron mesh roll. Yingyong Jichu yu Gongcheng Kexue Xuebao/Journal of Basic Science and Engineering 21(4):638–645
22. Su A, Su Y, Cheng H (2013) Effect of CO2/O2 on catalytic reduction of no by iron. Adv Mat Res 616–618:1849–1852
23. Lissianski VV, Zamansky VM, Maly PM (2001) Effect of metal-containing additives on nox reduction in combustion and reburning. Combust Flame 125(3):1118–1127
24. Su Y, Gathitu BB, Chen W-Y (2010) Efficient and cost effective reburning using common wastes as fuel and additives. Fuel 89(9):2569–2582. doi:10.1016/j.fuel.2009.12.009
25. Tsubouchi N, Ohtsuka Y (2008) Nitrogen chemistry in coal pyrolysis: catalytic roles of metal cations in secondary reactions of volatile nitrogen and char nitrogen. Fuel Process Technol 89(4):379–390. doi:10.1016/j.fuproc.2007.11.011
26. Illan-Gomez MJ, Linares-Solano A, Radovic LR, Salinas-Martinez de Lecea C (1995) NO reduction by activated carbons. 5 Catalytic effect of iron. Energy Fuels 9(3):540–548. doi:10.1021/ef00051a020
27. Wang Z, Zhou J, Wen Z, Liu J, Cen K (2007) Effect of mineral matter on NO reduction in coal reburning process. Energy Fuels 21(4):2038–2043. doi:10.1021/ef0604902
28. Dobrzański LA (1986) Metaloznawstwo i obróbka cieplna. Wydawnictwa Szkolne i Pedagogiczne, Warszawa
29. Tomeczek J, Gradoń B (1997) The role of nitrous oxide in the mechanism of thermal nitric oxide formation within flame temperature range. Combust Sci Technol 125(1–6):159–180. doi:10.1080/00102209708935658
30. Lissianski V, Zamansky V, Rizeq G (2002) Integration of direct combustion with gasification for reduction of NOx emissions. Proc Combust Inst 29(2):2251–2258. doi:10.1016/s1540-7489(02)80274-7
31. Werle S (2012) A reburning process using sewage sludge-derived syngas. Chem Pap 66(2):99–107. doi:10.2478/s11696-011-0098-y
32. Hill SC, Douglas Smoot L (2000) Modelling of nitrogen oxides formation and destruction in combustion systems. Prog Energy Combust Sci 26(4–6):417–458. doi:10.1016/s0360-1285(00)00011-3
33. Smoot LD, Hill SC, Xu H (1998) NOx control through reburning. Prog Energy Combust Sci 24(5):385–408. doi:10.1016/s0360-1285(97)00022-1
34. Al-Mansour F, Zuwala J (2010) An evaluation of biomass co-firing in Europe. Biomass Bioenergy 34(5):620–629. doi:10.1016/j.biombioe.2010.01.004
35. Samuelsen GS, Brouwer J, Vardakas MA, Holdeman JD (2013) Experimental and modelling investigation of the effect of air preheat on the formation of NOx in an RQL combustor. Heat Mass Transfer 49(2):219–231. doi:10.1007/s00231-012-1080-0
36. Fogler HS, Vennema A, Vennema C, Arbor A (2008) Elements of chemical reaction engineering. Pearson Education International, New Jersey
37. Tsotsas E, Schlünder EU (1990) Measurements of mass transfer between particles and gas in packed tubes at very low tube to particle diameter ratios. Wärme- und Stoffübertragung 25(4):245–256. doi:10.1007/bf01785411
38. Chen RY, Yeun WYD (2003) Review of the high-temperature oxidation of iron and carbon steels in air or oxygen. Oxid Met 59(5):433–468. doi:10.1023/a:1023685905159
39. Suárez L, Rodríguez-Calvillo P, Houbaert Y, Colás R (2010) Oxidation of ultra low carbon and silicon bearing steels. Corros Sci 52(6):2044–2049. doi:10.1016/j.corsci.2010.02.001
40. Sadakata M, Shigehisa T, Kunii D (1985) Development of a catalytic two-stage combustion system. AIChE J 31(5):767–772. doi:10.1002/aic.690310510
41. Sadakata M, Komiyama S, Sakai T (1985) Rapid Reduction of nitric oxide by hydrogen in the presence of stainless and Ni catalyst. Combust Sci Technol 44(3–4):195–205. doi:10.1080/00102208508960303
42. Sokolskii DV, Alekseeva GK, Khlystov AS, Yashkevich VI, Kotova GN (1977) Kinetics of nitric oxide reduction on Fe2O3/Al2O3 and the composition of the catalyst. React Kinet Catal Lett 6(1):59–64. doi:10.1007/bf02067740
43. Randall H, Doepper R, Renken A (1998) Reduction of nitrogen oxides by carbon monoxide over an iron oxide catalyst under dynamic conditions. Appl Catal B 17(4):357–369. doi:10.1016/s0926-3373(98)00021-6
44. Randall H, Doepper R, Renken A (1997) Modelling CO oxidation on silica-supported iron oxide under transient conditions. Ind Eng Chem Res 36(8):2996–3001. doi:10.1021/ie960613d
45. Kær SK (2004) Numerical modelling of a straw-fired grate boiler. Fuel 83(9):1183–1190. doi:10.1016/j.fuel.2003.12.003
46. Yin C, Rosendahl LA, Kær SK (2008) Grate-firing of biomass for heat and power production. Prog Energy Combust Sci 34(6):725–754. doi:10.1016/j.pecs.2008.05.002
47. Houshfar E, Skreiberg Ø, Todorović D, Skreiberg A, Løvås T, Jovović A, Sørum L (2012) NOx emission reduction by staged combustion in grate combustion of biomass fuels and fuel mixtures. Fuel 98:29–40. doi:10.1016/j.fuel.2012.03.044
48. Abuluwefa H, Guthrie R, Ajersch F (1997) Oxidation of low carbon steel in multicomponent gases: part I. Reaction mechanisms during isothermal oxidation. Metall Mat Trans A 28(8):1633–1641. doi:10.1007/s11661-997-0255-7